Indian Journal of Chemical Technology
Vol. 31, September 2024, pp. 762-769
DOI: 10.56042/ijct.v31i5.5886

Visible light driven g-C_3N_4 photocatalytic pretreatment of rice straw for enhanced biogas production

R Tamilselvan & A. Immanuel Selwynraj*
School of Mechanical Engineering, Vellore Institute of Technology, Vellore, India
*E-mail: aisraj1979@gmail.com

Received 28 September 2023; accepted 11 July 2024

This study investigates the utilization of Graphitic Carbon Nitride (g-C_3N_4) as a photocatalytic material for enhancing biofuel production from rice straw, an agricultural residue with potential for sustainable energy generation. The melamine-synthesized g-C_3N_4 is used as a pretreatment agent, where rice straw is immersed in a g-C_3N_4 solution and exposed to 450-600 nm solar irradiation for varying durations. This pretreatment process modifies the biomass structure, resulting in a reduction of the silica content to 72.05% and an increase in the carbon percentage to 41.58% within the rice straw. Methane production demonstrates the effectiveness of g-C_3N_4-based pretreatment, with methane production from raw rice straw at 231 mL/g_{VS}. Co-digestion with waste activated sludge increases methane production to 507 mL/g_{VS}, while a 3 h pretreatment further enhances it to 547.16 mL/g_{VS}, and a 6 h pretreatment leads to 595.5 mL/g_{VS}. Comprehensive characterization techniques confirm the successful modification of biomass structure using g-C_3N_4.

Keywords: Biogas, Oxidation, Photocatalyst, Pretreatment, Silica Removal

Introduction

Bio-energy is eco-friendly due to its carbon-neutral properties[1]. The annual worldwide production of rice straw is estimated to be approximately 800–1000 million tons (MT), with Asia accounting for nearly 90% of the total output of 600–800 MT[2]. However, farmers are compelled to burn rice straw in the fields themselves due to limited economically viable alternatives for its utilization[3]. In India, approximately 16% of crop residues, with 60% being rice straw, are burned in the fields[4]. The combustion of 1 kg of rice straw releases approximately 0.019–0.069 g of NOx and 0.7–4.51 g of CH_4, along with the production of toxic gases such as CO, SO_2, and volatile organic compounds (VOCs), posing environmental and human health hazards[5]. To mitigate the adverse effects associated with the burning of rice straw, its utilization for the production of second-generation biofuels is recommended. With its abundant carbon resources, rice straw is well-suited for this purpose. Anaerobic digestion provides a means to effectively utilize a substantial quantity of rice straw for biogas production, thereby contributing to the reduction of greenhouse gas emissions[6]. Despite the energy potential, widespread availability, and low cost of rice straw as a resource, it remains underutilized due to its complex physical structure, particularly the significant presence of silica within the biomass structure. This high silica content hinders efficient access to the energy content during the biofuel production process[7]. Thus, pretreatment is essential to enhance its suitability for anaerobic digestion by breaking down the recalcitrant structure, facilitating improved access of microorganisms to the targeted chemicals for CH_4 production.

Photocatalytic technology is an emerging technology that has been developed over the past few decades[8]. Semiconductor photocatalysts are extensively used for degrading pollutants due to their applications in self-cleaning, dye degradation, water purification, and sensing. For an instance, Ming *et al*. employed a photocatalytic nanocomposite of TiO_2-ZnO to pretreat lignin with the goal of generating methane. The pretreated lignin using TiO_2-ZnO exhibited a notable increase of around 39% in methane production[9]. An advanced oxidation process using UV irradiation and TiO_2 was applied to wheat straw to increase its biodegradability for enhanced biogas production by anaerobic digestion. The focus was on oxidizing the lignin in the straw to release sugars from the lignocellulosic structure. Different TiO_2 concentrations and irradiation times were tested, and lignin oxidation products were quantified. The most effective pretreatment condition was subsequently evaluated in continuous mode of reaction, leading to a 37% increase in CH_4 yield[10].

Photocatalysis with semiconductors like titanium dioxide shows significant potential in this area. Nevertheless, interest has surged in alternative photocatalysts that may provide comparable or even enhanced performance due to limitation of TiO_2 to absorb only UV light, which constitutes a small segment (100–400 nm) of the solar spectrum. This limitation reduces their efficiency, as they need UV light sources or sunlight with UV radiation to function effectively[11]. Thus, there's a need for innovative materials that are active under visible light and display high pretreatment efficiency. In this study, a g-C_3N_4 photocatalyst was synthesized employing Melamine as a precursor through a thermal polycondensation process. It exhibits activation under visible light conditions.g-C_3N_4 is selected for photocatalytic treatment due to its superior ability to harness visible light, coupled with high stability, efficient charge separation, ample surface area, and surpassing traditional photocatalysts like TiO_2 and ZnO, which typically require UV light and are prone to rapid charge recombination. Melamine is chosen as a precursor for synthesizing g-C_3N_4 because of its high nitrogen content, which enhances the electronic properties of the photocatalyst, promotes effective charge separation, and enhances its efficiency for visible light photocatalysis compared to traditional catalysts like TiO_2[(Ref.12)]. The treated samples structure and morphology were analysed. This method effectively breaks down the lignin structure of rice straw by removing silica and making it more suitable for further processing. This study provides an insight on g-C_3N_4 application in rice straw pretreatment, which has never been reported.

Experimental Section

The rice straw was collected from a local farming land and grounded into 0.5-0.7 mm powder. It was then dried in an oven at 60°C for 2 h to remove excess moisture. Melamine ($C_3H_6N_6$) was utilized as a precursor for the synthesis of g-C_3N_4 through the thermal polycondensation process. The melamine was subjected to a temperature of 550°C in a furnace for 5.30 h, resulting in the formation of two-dimensional polymer Graphitic carbon nitride (g-C_3N_4). The FESEM microstructure of g-C_3N_4 and EDX analysis is shown in Fig. 1 and Fig. 2, confirming the proper formation of g-C_3N_4 for subsequent applications. In a 500 mL beaker, 1 g of the synthesized catalyst was mixed with 300 mL of water using a magnetic stirrer for 6 h to achieve a homogeneous solution. The RS was immersed in this solution and treated for various time intervals, including 1 h, 3 h, 6 h, and 10 h. The solution containing the samples was exposed to sunlight, with a solar irradiation at a wavelength of 450-600 nm. At the end of each time interval, samples were collected and washed with distilled water to remove any residual g-C_3N_4 particles. This step is crucial as g-C_3N_4 possesses antibacterial properties that may affect the microbes during biofuel production. Following these processes, the treated samples underwent different characterization tests to ensure their photocatalytic effectiveness. These tests included UV-visible spectroscopy, FESEM, XRD, EDX, and FTIR.

Results and Discussion

Mechanism of pretreatment

Catalyst activation

The g-C_3N_4 photocatalyst can be activated under solar irradiation by absorbing photons, which leads to the generation of electron-hole pairs in the conduction band (CB) and valence band (VB) of the material. The electrons (e^-) in the CB and the holes (h^+) in the VB subsequently react with oxygen and water,

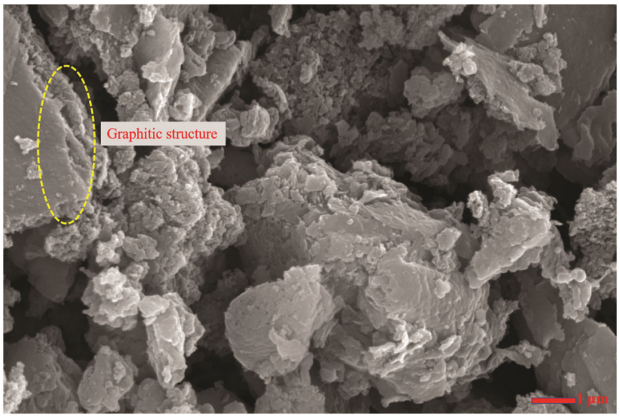

Fig. 1 — FESEM image of g-C_3N_4 photocatalyst

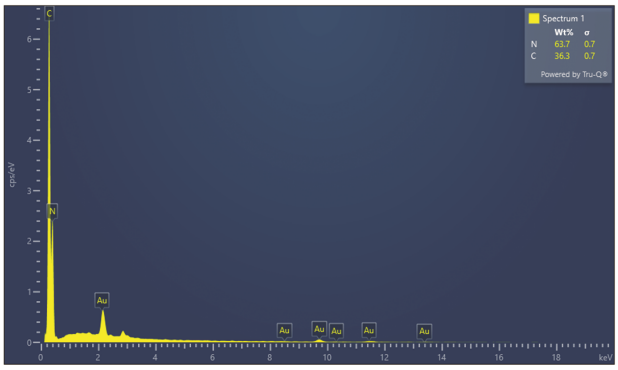

Fig. 2 — EDX compositional analysis of g-C_3N_4

respectively (Eq. (1)). This results in the formation of negatively charged oxygen radical (O_2^-•) and hydroxyl radical (OH•) (Eqs (2&3)).

$$g\text{-}C_3N_4 + h\nu \rightarrow e^- (CB) + h^+(VB) \quad \ldots (1)$$

$$e^- + O_2 \rightarrow O_2^-\bullet \quad \ldots (2)$$

$$h^+ + H_2O \rightarrow OH\bullet + H^+ \quad \ldots (3)$$

Biomass degradation

Once activated by solar irradiation, the photocatalyst generates electron-hole pairs (e^-/h^+), which initiate a series of complex reactions with the rice straw constituents. The lignin fraction in rice straw undergoes degradation upon interaction with the photocatalyst. The catalytic activity of the electron (e^-) leads to the breakdown of lignin into degraded lignin fragments, including phenolic compounds and aromatic structures. These degraded lignin products arise from the cleavage of various chemical bonds present in the lignin structure. Similarly, the cellulose fraction in rice straw experiences degradation through the photocatalytic process. The e^- from the photocatalyst engages with cellulose, resulting in the formation of degraded cellulose fragments. These fragments consist of glucose and other sugar monomers, which arise from the cleavage of glycosidic linkages in the cellulose structure. Moreover, hemicellulose, another constituent of rice straw, undergoes degradation when subjected to photocatalytic treatment. The e^- interacts with hemicellulose, leading to the formation of degraded hemicellulose fragments. These fragments comprise a variety of sugar monomers and oligosaccharides, resulting from the cleavage of glycosidic linkages within the hemicellulose structure. The photocatalytic degradation of lignin, cellulose, and hemicellulose in rice straw result in the generation of fragmented products with altered chemical structures. These degraded products exhibit a reduced molecular weight compared to their original counterparts, facilitating their subsequent conversion during anaerobic digestion.

Mechanism of silica reduction

The presence of silica and lignin in rice straw acts as a protecting layer for its carbohydrates, causing challenges in hydrolysis of substrate in anaerobic digestion and silica not only acts as a physical barrier, but it also inhibits hydrolytic enzymes[13]. Additionally, it can lead to the formation of harmful gases like hydrogen sulphide during anaerobic digestion, impacting biogas quality. Khaleghian *et al.* [14] revealed that the protective impact of the silica layer exceeded that of the lignin within RS. When $g\text{-}C_3N_4$ is applied as a catalyst in the presence of light and reactive species like hydroxyl radicals (OH•), it can facilitate reactions that lead to the breakdown of silica (SiO_2) into silicate ions (SiO_4^{4-}), as shown in the Eq. 4 and Eq. 5. $g\text{-}C_3N_4$ generates electron-hole pairs upon light exposure, facilitating redox reactions that activate oxygen molecules and hydroxyl radicals. As a result, $g\text{-}C_3N_4$ enhances the transformation of silica into silicate ions, potentially lowering the silica content in rice straw. The decrease in silica content was assessed through XRD, FESEM, and EDX analyses.

$$OH\bullet + SiO_2 \rightarrow SiO_4^{4-} + H_2O \quad \ldots (4)$$

$$O_2^{-}\bullet + SiO_2 \rightarrow SiO_4^{4-} + O_2 \quad \ldots (5)$$

Photocatalytic reduction of silica

The reduction of silica in rice straw was assessed by FESEM micrograph and EDX analysis for pretreatment efficacy at varying intervals. Structures identified in raw rice straw during FESEM analysis include Si cubic bodies, ladder-like structures, and trichomes, as shown in Fig. 3(a). Magnified images (10 μm) of rice straw under different pretreatment conditions are shown in Fig. 3(b) and Fig. 4 (a & b). This study aimed to optimize the main product (Si) from photocatalytic treatment by irradiating biomass for 1, 3, 6, and 10 h with 1 g catalyst for 50 g rice straw in 300 mL water. In Fig. 3(a), the microstructure of untreated rice straw reveals the complete coverage of the biomass surface by silica bodies. Following 1 h pretreatment, the silica bodies exhibit slight degradation, yet the underlying structure remains unchanged (Fig. 3 (b)). After 3 h of treatment, significant degradation of the silica bodies becomes evident, although the overall structure of silica remains robust (Fig.4 (a)). With a 6 h treatment duration, a substantial disintegration of the silica bodies' surface is observed, indicating that a 6 h treatment period is effective in facilitating silica reduction (Fig. 4(b)).

The EDX analysis revealed the elemental composition of rice straw samples. It indicated that the untreated rice straw contains 22.8% Si, with carbon and oxygen percentages of 28.5% and 46.9%, respectively (Table 1). The higher is the silica content in rice straw's internal structure more is the resistance to the enzymatic hydrolysis. The low carbon and high oxygen content leads to inhibit the gas yield. The results showed that after 3 h of treatment, silica decreased to 18% and carbon increased to 38.5%.

Similarly, after 6 h, carbon further increased to 48% and silica decreased to 6.4% (Table 1). The increase in carbon content is attributed to the removal of silica and hemicellulose, while cellulose is retained in the pretreated rice straw.

Additionally, pretreated rice straw had chlorine content of 0.5%, significantly lower than untreated rice straw (approximately 1% chlorine). Chlorine inhibits microbial growth during anaerobic digestion. The findings suggest that the photocatalytic treatment substantially alters rice straw's chemical composition by reducing silica and increasing carbon, leading to improved biogas yield and composition, and reduced inhibition of microbial growth during anaerobic digestion. Furthermore, EDX analysis after 10 h showed the carbon content increased to 49% and silica decreased to 6%. However, there is no significant changes between 6 h and 10 h pretreatment. Hence, additional 4 h may not be necessary.

Table 1 — EDX analysis of RS at different pretreatment conditions

Elemental Composition	Raw rice straw (%)	3 h treated rice straw (%)	6 h treated rice straw (%)
Carbon (C)	28.5	38.54	48.02
Oxygen (O)	46.87	42.6	43.61
Silica (Si)	22.84	18.05	6.39
Chlorine (Cl)	0.96	0.4	0.51
Calcium (Ca)	0	0.41	0.98

The energy band gap of g-C_3N_4, as depicted in the Fig. 5, is approximately 2.7 eV, enabling the utilization of visible light up to a wavelength of 460 nm. To determine the band gap of the g-C_3N_4 photocatalyst, Kubelka-Munk and Tauc plots were employed. The energy gap value (E_g) was calculated using the following Eq. 6.

$$\alpha h\upsilon = \beta (h\upsilon - E_g)^n \quad \ldots (6)$$

where α represents the absorption coefficient, β denotes the absorption constant, λ is the wavelength

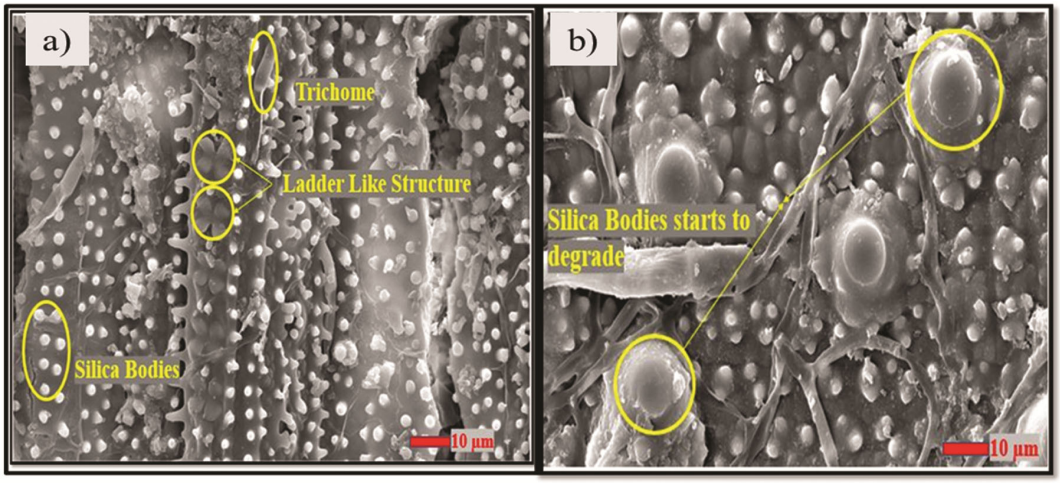

Fig. 3 — SEM micrographs of (a) raw and (b) 1 h treated rice straw

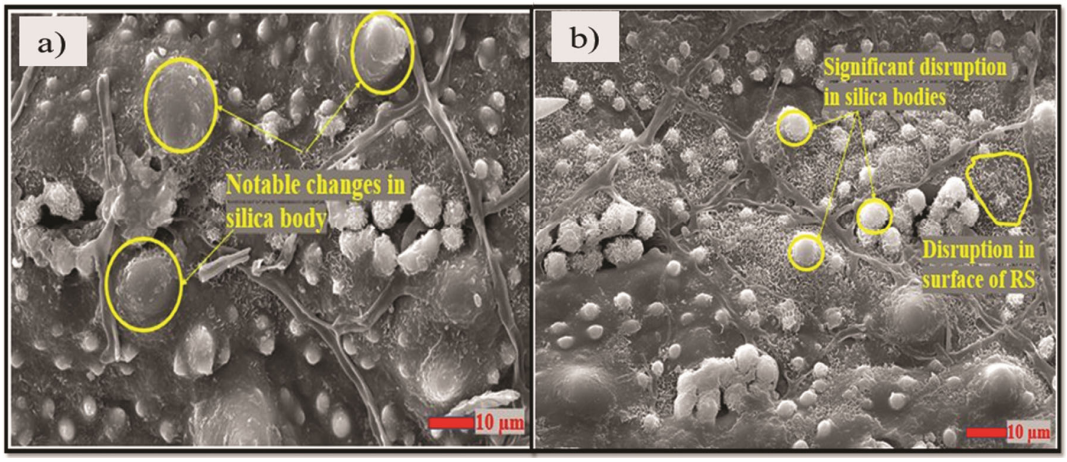

Fig. 4 — SEM micrographs of (a) 3h and (b) 6 h treated rice straw (RS)

of light, and η signifies the energy threshold. The CB and VB positions of g-C_3N_4 are -1.1 eV and +1.6 eV, respectively, relative to the normal hydrogen electrode, meeting photocatalytic requirements and increasing the production of electron-hole pairs[15].

XRD characterization of g-C_3N_4

The XRD technique was employed to determine the crystal structure and lattice constant and of g-C_3N_4. The obtained XRD pattern exhibited distinct peaks at 13° and 27°, corresponding to the (100) and (002) diffraction planes, respectively, which are characteristic of graphitic materials (JCPDS 87-1526)[16]. Fig. 6 depicts the peak intensity of g-C_3N_4 before and after treatment. The observed peak intensities exhibit negligible changes, indicating the retention of the structure of the photocatalyst, even after multiple uses. The XRD analysis clearly reveals the flake-like structure of g-C_3N_4, as evidenced by the (002) diffraction peak, which corresponds to an interplanar stacking distance of 0.325 nm. This value is comparable to the stacking distance of graphite, which is 0.34 nm. The similarity in interplanar spacing further supports the graphitic nature of g-C_3N_4.

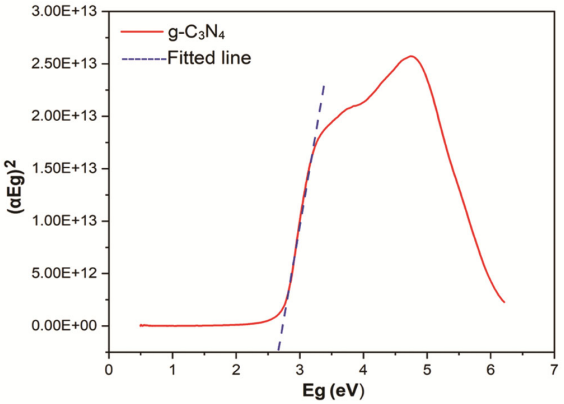

Fig. 5 — Tauc plot of g-C_3N_4

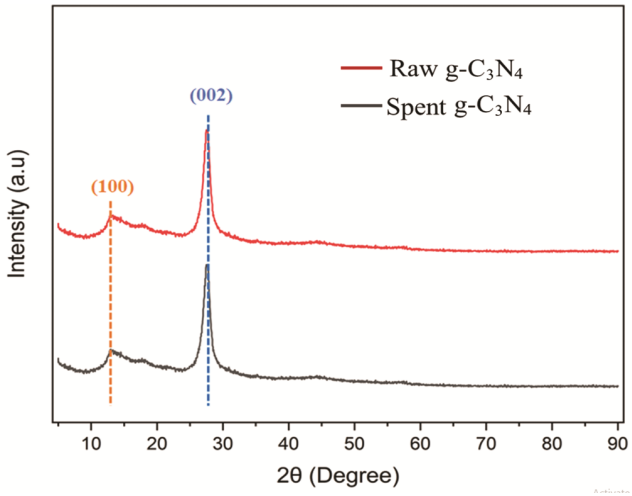

Fig. 6 — XRD pattern of g-C_3N_4

Crystallinity change of rice straw

Fig. 7 illustrates that the untreated biomass exhibits characteristic cellulose peaks at angles of 15° and 22.1°. These peaks correspond to the lattice planes of crystalline cellulose I, specifically the (001) and (002) planes[17]. Due to higher van der Waals interactions existing between the hydrogen-bonded layers of cellulose I in contrast to cellulose II, cellulose I demonstrates heightened resistance to cellulose hydrolysis. After the treatment, a noticeable shift of the highest peak (221) to 21.2° indicates that the amorphousness of cellulose I increased and it got transformed into cellulose II. The reduction in peak intensity, as confirmed by FESEM-EDX analysis, provides evidence of a decrease in silica content in the rice straw due to the amorphization of cellulose. This structural modification is attributed to the presence of reactive oxygen species (ROS) like hydroxyl radicals (OH•) and these radicals react with cellulose, causing bond cleavage and disrupting the ordered structure, resulting in increased amorphousness[15]. The decrease in intensity of the peak at 15° indicates a higher degree of cellulose degradation during the treatment.

Functional group characterization of g-C_3N_4

The FTIR spectra of g-C_3N_4, as depicted in the Fig. 8, exhibit characteristic peaks within the wavenumber range of 800 to 1650 cm^{-1}. These peaks are indicative of the stretching vibrations exhibited by repeating units derived from aromatic heptazine compounds. Notably, they include the distinctive

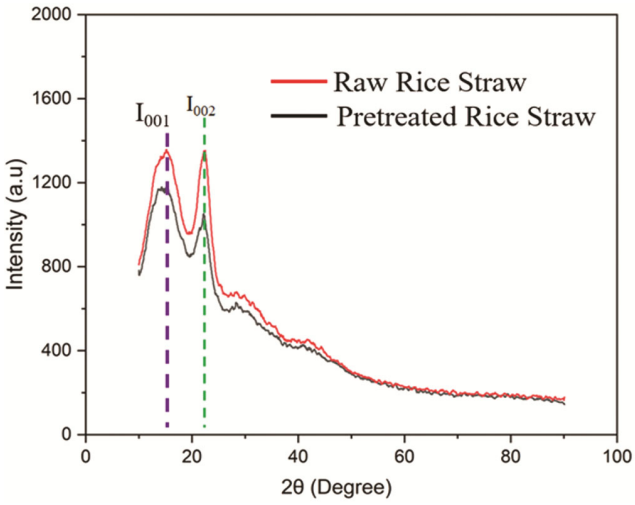

Fig. 7 — XRD pattern of treated and non-treated rice straw

stretching modes of sp^2 C═N bonds and the out-of-plane bending vibrations of sp^3 C─N bonds[12]. Within the spectral range of approximately 810 cm^{-1}, a prominent peak is observed, representing the breathing mode of the triazine unit. Intense peaks observed in the range of 3000-3400 cm^{-1} were attributed to the stretching vibrations of residual free groups, specifically O-H and N-H. The Raman spectra recorded for g-C_3N_4 exhibited distinct peaks at wavenumbers of 807, 1246, 1410, 1575, 1638, 3070, and 3330 cm^{-1}.These peaks corresponded to specific vibration modes associated with the CN heterocycle present in g-C_3N_4.The observed shift at 1246 cm^{-1} is attributed to phonon confinement and the remarkable quantum confinement effect.

Functional group characterization of rice straw

After pretreatment with g-C_3N_4, notable changes were observed in the FTIR analysis of rice straw as shown in Fig. 9. The O-H stretching peak increased from 3242 cm^{-1} to 3350 cm^{-1}, indicating the enhanced hydrogen bonding. The C=C-H peak decreased significantly from 2900-2700 cm^{-1}, indicating a decrease in unsaturation. The C-H peak intensity reduced from 2600 cm^{-1} to 2400 cm^{-1}, representing that the decrease in aliphatic groups. The C=C peak decreased from 1629 cm^{-1} to 1515 cm^{-1}, indicating the decrease in aromatic compounds. The C-O-C peak reduced from 1054 cm^{-1} to 1029 cm^{-1}, reflecting a decrease in glycolic bond and C-O-C ring skeleton vibration. The Si-O-Si peak reduced from 772 cm^{-1} to 663 cm^{-1}, indicating a decrease in silica content. These changes show that the significant structural modifications in the pretreated rice straw sample.

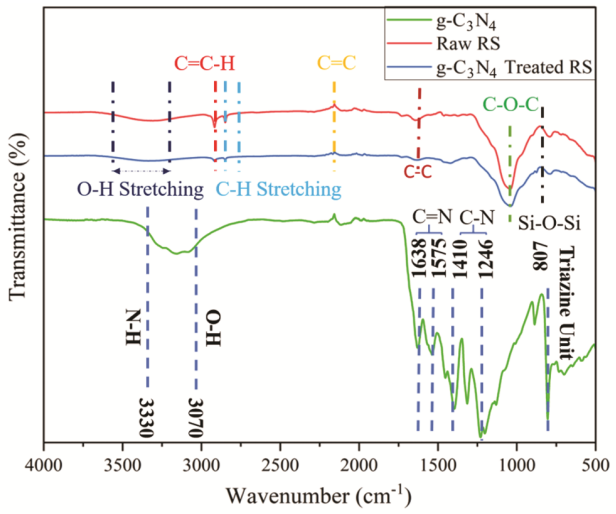

Fig. 8 — FTIR spectra of (a) treated and (b) non-treated rice straw (RS)

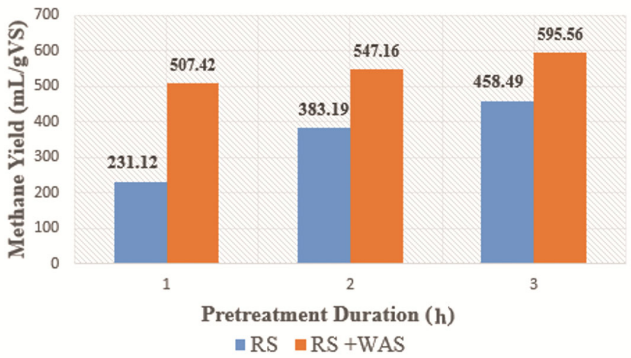

Fig. 9 — Methane yield before and after pretreatment

Influence of pretreatment on biogas production

The modified rice straw, characterized by reduced silica content and enhanced carbon content, undergoes anaerobic digestion to initiate the production of biogas. During this process, the rice straw was fermented by methanogenic microorganisms, leading to the production of biogas, primarily methane (CH_4) and carbon dioxide (CO_2). The overall fermentation reactions, highlighting the influence of silica reduction and carbon enhancement, can be represented as Eqs 6 & 7.

Cellulose hydrolysis and methane production:

$$C_6H_{10}O_5 \longrightarrow C_6H_{12}O_6 \longrightarrow 3CH_4 + 3CO_2 \quad \ldots (7)$$

Hemicellulose degradation and methane formation:

$$(C_5H_8O_4)n \longrightarrow C_5H_{10}O_5 \longrightarrow \text{Methane and Carbon dioxide} \quad \ldots (8)$$

The reduction in silica content and enhancement of carbon content in the rice straw through the g-C_3N_4 pretreatment positively impact the biogas yield. Silica, being an inert component, does not contribute significantly to the biogas production[18]. The available carbon fraction in the rice straw increases by reducing the silica content. This increased carbon availability enhances the substrate accessibility for the methanogenic microorganisms during anaerobic digestion, resulting in improved biogas production.

The stoichiometric approach developed by Buswell (Eq. 8) enables the estimation of methane quantity based on the elemental composition of the treated rice straw[19,20]. The model aims to facilitate the estimation of biogas potential of treated substrate and serves as an alternative to physical anaerobic digesters. To ensure the availability of microorganisms in the anaerobic process, waste activated sludge was co-digested with rice straw in a 1:1 ratio.

$$C_aH_bO_cN_d + [\,4a-b-2c+3d\,/\,4]\,H_2O \rightarrow [4a+b-2c-3d\,/\,8]\,CH_4 + [\,4a-b+2c+3d\,/\,8]\,CO_2 + dNH_3 \quad \ldots (9)$$

According to the model, methane production from raw rice straw was 231 mL/g_{VS}. When co-digested with waste activated sludge, methane production increased to 507 mL/g_{VS}. After a 3 h pretreatment, the production further increased to 547.16 mL/g_{VS}, and after a 6 h pretreatment, it reached 595.5 mL/g_{VS} (Fig. 9). Kang and Kim (2011) also observed this phenomenon by pre-treating the rice straw using only UV-light in the absence of TiO_2[21]. However, regardless of the catalyst dose, irradiating the straw for an hour did not lead to a significant increase in methane yield. This is due to the limited exposure time, which is not sufficient to induce a significant change in the biomass structure.

These results suggest that the duration of the pretreatment process is a critical factor in determining the biomethane potential of rice straw. However, extending the pretreatment duration beyond a certain point may not result in any significant increase in the biomethane potential. Therefore, the pretreatment duration should be optimized to achieve maximum biomethane potential while minimizing the energy and resource consumption associated with the pretreatment process. Moreover, the study also highlights the importance of selecting an appropriate photocatalyst dosage for effective pretreatment. The addition of g-C_3N_4 to the pretreatment process resulted in an increase in the biomethane potential of rice straw. However, the effect of the photocatalyst on the biomethane potential was not linear, and the optimal dosage needs to be carefully determined through further experiments.

Biogas potential test

To assess the efficacy of catalyst loading in the pretreatment process, a laboratory-scale anaerobic digestion experiment was conducted. A custom 1 L anaerobic digester with a working volume of 800 mL was utilized, and it was supplied with 100 g of finely ground rice straw (0.5-0.7 mm). Despite being pretreated, rice straw undergoing mono digestion fails to generate an adequate amount of microorganisms responsible for hydrolysis due to its high carbon to nitrogen ratio [22]. Consequently, anaerobic sludge (Inoculum) from the pre-existing digester is introduced into the current digester at a dosage of 10 g .This straw had been pretreated using catalyst loadings of 0.5% and 1% (w/w) g-C_3N_4. The initial

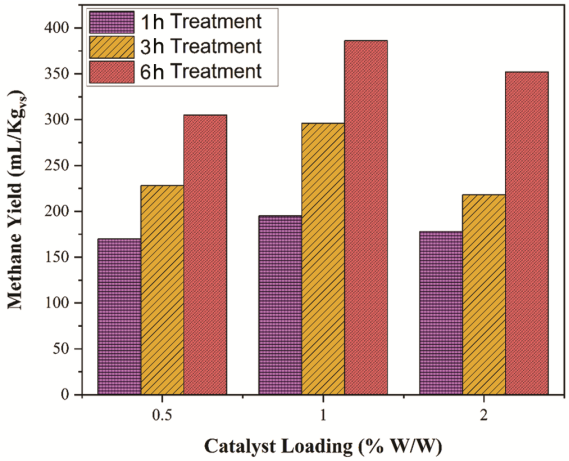

Fig. 10 — Catalyst loading *vs* methane production

organic loading rate of the digester was consistently maintained at 15 g/L, while methane yield was calculated. Concurrently, the catalyst loading rate was increased to 1-2% (w/w) g-C_3N_4, all while maintaining the same organic loading rate. Both digesters were subjected to irradiation at 1, 3, and 6 h of pretreatment. The cumulative methane yield for various irradiation time intervals is depicted in Fig. 10. The results indicate a noteworthy enhancement in methane yield when the catalyst loading rate was elevated from 0.5 to 1% (w/w) g-C_3N_4. Additionally, the duration of irradiation time exhibited a significant influence on the process. Notably, a 6 h pretreatment duration yielded the highest methane output of 386 mL/g_{VS} at 1% (w/w) g-C_3N_4, representing a 21% increase over the 0.5% (w/w) g-C_3N_4 loading. Surprisingly, when the catalyst loading rate was increased to 2% (w/w) g-C_3N_4, there was no substantial enhancement in methane yield; in fact, the methane yield plummeted to 0.8% after 6 h of pretreatment. These observations collectively lead to the conclusion that a 1% (w/w) g-C_3N_4 loading rate serves as the optimal condition for achieving superior biogas production during anaerobic digestion. It is evident that this percentage marks the threshold loading rate. Furthermore, in the investigation conducted by Ye *et al*. (2013), it was unveiled that raw rice straw, in conjunction with an inoculum, produces 205 mL/g_{VS} of methane[23]. Consequently, the current study show cases the potential of photocatalytic pretreatment to bolster biogas production.

Conclusion

Successful synthesis of g-C_3N_4 using the thermal polycondensation method has vividly showcased its

potential for efficiently degrading rice straw under visible light. The optimal pretreatment duration, established at 6 h, yielded a substantial 72.05% reduction in silica content and a notable 41.58% enhancement in carbon composition. These significant outcomes were corroborated by the FESEM-EDS analysis, which provided compelling evidence of the alterations in both silica content and carbon structure. Furthermore, XRD and FTIR studies further verified the effectiveness of g-C_3N_4 pretreatment. The pinnacle of the biogas yield, amounting to 386 mL/g_{VS}, was achieved through a 1% (w/w) g-C_3N_4 loading rate and a 6 h irradiation time during the pretreatment. This configuration is proven to be the optimum and effective loading rate for enhancing the photocatalytic reforming of rice straw. These results present a promising trajectory for future research, underscoring the potential prowess of g-C_3N_4 in rice straw pretreatment as a means to elevate biofuel production.

References

1 Morya R, Andrianantenaina F H, Singh S, Pandey A K, Gi-Beom K, Verma J P, Kumar G, Raj T & Sang-Hyoun K, Exploring rice straw as substrate for hydrogen production: Critical challenges and opportunities, *Environ Technol Innov*, 31 (2023) 103153.

2 (IRRI) International Rice Research Institute, World Rice Statistics, available from: http://ricestat.irri.org:8080/wrsv3/entrypoint.html (2022).

3 Mahajan S M, Salunkhe S K, Mahadik A A & Gharat S H, Cavitation based pretreatment of biomass for intensification of biogas production, *Indian J Chem Technol*, 29 (2022) 459.

4 Bhattacharyya P, Bisen J, Bhaduri D, Priyadarsini S, Munda S, Chakraborti M, Adak T, Panneerselvam P, Mukherjee A K, Swain S L, Dash P K, Padhy S R, Nayak A K, Kumar S & Nimbrayan P, Turn the wheel from waste to wealth: Economic and environmental gain of sustainable rice straw management practices over field burning in reference to India, *Sci Total Environ*, 775 (2021) 145896.

5 Nguyen V H, Sander B O, Quilty J R, Balingbing C, Grace C A, Romasanta R, Alberto M C R, Sandro J M, Jamieson C & Gummert M, An assessment of irrigated rice production energy efficiency and environmental footprint with in-field and off-field rice straw management practices, *Sci Rep*, 9 (2019) 1.

6 Enock T K, King'ondu C K, Pogrebnoi A & Jande Y A C, Biogas-slurry derived mesoporous carbon for supercapacitor applications, *Mater Today Energy*, 5 (2017) 12.

7 Van-Soest P J, Rice straw, the role of silica and treatments to improve quality, *Anim Feed Sci Technol*, 130 (2006) 137.

8 Lan Y, Wang Y, Guan Y, Du L & Lv Y, Synthesis and photocatalytic activity of g-C_3N_4/$BiVO_4$/CNTs composites, *Mater Lett*, 330 (2023) 133359.

9 Chu Y M, Javed H M A, Awais M, Khan M I, Shafqat S, Khan F S, Mustafa M S, Ahmed D, Khan S U & Khalil R M A, Photocatalytic pretreatment of commercial lignin using TiO_2-ZnO nanocomposite-derived advanced oxidation processes for methane production synergy in lab scale continuous reactors, *Catalysts*, 11 (2021) 54.

10 Alvarado-Morales M, Tsapekos P, Awais M, Gulfraz M & Angelidaki I, TiO_2/UV based photocatalytic pretreatment of wheat straw for biogas production, *Anaerobe*, 46 (2017) 155.

11 Lin L & Ali K A, Photocatalytic degradation of organic compounds in dye wastewater by Fe^{3+} doped nano-ZnO/TiO_2 composite photocatalyst, *Indian J Chem Technol*, 31 (2024) 506.

12 Wen J, Xie J, Chen X & Li X, A review on g-C_3N_4-based photocatalysts, *Appl Surf Sci*, 391 (2017) 72.

13 Van-Soest P J, Rice straw, the role of silica and treatments to improve quality, *Anim Feed Sci Technol*, 130 (2006) 137.

14 Khaleghian H, Molaverdi M & Karimi K, Silica removal from rice straw to improve its hydrolysis and ethanol production, *Ind Eng Chem Res*, 56 (2017) 9793.

15 Singh P P & Srivastava V, Recent advances in visible-light graphitic carbon nitride (g-C_3N_4) photocatalysts for chemical transformations, *RSC Adv*, 12 (2022) 18245.

16 Wang X, Maeda K, Thomas A, Takanabe K, Xin G, Carlsson J M, Domen K & Antonietti M, A metal-free polymeric photocatalyst for hydrogen production from water under visible light, *Nat Mater*, 8 (2008) 76.

17 Cheng G, Varanasi P, Li C, Liu H, Melnichenko Y B, Simmons B, Kent M & Singh S, Transition of cellulose crystalline structure and surface morphology of biomass as a function of ionic liquid pretreatment and its relation to enzymatic hydrolysis, *Biomacromolecules*, 12 (2011) 933.

18 Pal P, Li H & Saravanamurugan S, Removal of lignin and silica from rice straw for enhanced accessibility of holocellulose for the production of high-value chemicals, *Bioresour Technol*, 361 (2022) 127661.

19 Achinas S & Euverink G J W, Theoretical analysis of biogas potential prediction from agricultural waste, *Resour Effic Technol*, 2 (2016) 413.

20 Buswell A M & Hatfeld W D, Anaerobic fermentations, *State Ill Dept Regist Educ Div. State Water Survey*, *Urbana Ill* (1936).

21 Kang H K & Kim D, Efficient bioconversion of rice straw to ethanol with TiO_2/UV pretreatment, *Bioproc Biosyst Eng*, 35 (2011) 43.

22 Jha B, Isha A, Trivedi A, Chandra R & Subbarao P M V, Anaerobic co-digestion of rice straw and de-oiled rice bran for biomethane production, *Energy Rep*, 7 (2021) 704.

23 Ye J, Li D, Sun Y, Wang G, Yuan Z, Zhen F & Wang Y, Improved biogas production from rice straw by co-digestion with kitchen waste and pig manure, *Waste Manag*, 33 (2013) 2653.